# Evidence for a larger contribution of smoldering combustion to boreal forest fire emissions from tower observations in Alaska

Elizabeth B. Wiggins[1], Arlyn Andrews[2], Colm Sweeney[2], John B. Miller[2], Charles E. Miller[3], Sander Veraverbeke[4], Roisin Commane[5], Steve Wofsy[6], John M. Henderson[7], and James T. Randerson[1]

[1]Department of Earth System Science, University of California, Irvine, California, USA, [2]National Oceanic and Atmospheric Administration, Boulder, Colorado, USA, [3]Jet Propulsion Laboratory, California Institute of Technology, Pasadena, California, USA, [4]Vrije University Amsterdam, Netherlands, [5]Department of Earth and Environmental Sciences, Columbia University, Palisades, New York, USA, [6]School of Engineering and Applied Sciences, Harvard, Cambridge, Massachusetts, USA, [7]Atmospheric and Environmental Research, Inc., Lexington, Massachusetts, USA,

*Correspondence to:* Elizabeth B. Wiggins (Elizabeth.b.wiggins@nasa.gov)

**Abstract.** With recent increases in burned area within boreal forests that have been linked to climate warming, there is a need to better understand the composition of emissions and their impact on atmospheric composition. Most previous studies have estimated boreal fire emission factors from daytime samples collected via aircraft near fire plumes or at the surface near actively burning fires. Here we quantified emission factors for CO and $CH_4$ from a massive regional fire complex in interior Alaska during the summer of 2015 using continuous high-resolution trace gas observations from the CRV tower (Fox, AK). Averaged over the 2015 fire season, the $CO/CO_2$ emission ratio was $0.138 \pm 0.048$ and the CO emission factor was $145 \pm 50$ g CO per kg of dry biomass consumed. The $CO/CO_2$ emission ratio was about 35% higher and more variable than most previous aircraft-based estimates for fresh wildfire emissions. The mean $CH_4/CO_2$ emission ratio was $0.010 \pm 0.003$ and the $CH_4$ emission factor was $6.05 \pm 2.09$ g $CH_4$ per kg of dry biomass consumed, with means similar to previous reports. CO and $CH_4$ emission factors varied in synchrony, with higher $CH_4$ emission factors observed during periods with lower modified combustion efficiency (MCE). By coupling a fire emissions inventory with an atmospheric model, we identified that at least 35 individual fires contributed to trace gas variations measured at the CRV tower, representing a significant increase in sampling compared to the number of boreal fires measured in all previous boreal forest fire work. The model also indicated that typical mean transit times between trace gas emission and tower measurement were 1-3 days, indicating that the time series sampled combustion across day and night burning phases. The high and variable CO emission factor estimates reported here provide evidence for a more prominent role of smoldering combustion, highlighting the importance of continuously sampling of fires across time-varying environmental conditions that are representative of typical burning conditions.

## 1 Introduction

Boreal forest fires influence the global carbon cycle and climate system through a variety of pathways. Boreal forest fires initiate succession, influence landscape patterns of carbon accumulation, and directly release carbon dioxide and other trace gases into the atmosphere [*Johnson*, 1996]. One of the largest reservoirs of global terrestrial carbon resides in organic soils underlying boreal forests [*Apps et al.*, 1993; *McGuire et al.*, 2010], and fires in the boreal forest can consume significant amounts of aboveground and belowground biomass [*Harden et al.*, 2000; *French et al.*, 2004; *Boby et al.*, 2010; *Walker et al.*, 2018]. Many boreal forest fires are stand replacing and high energy [*Rogers et al.*, 2015], with enough convective power to inject smoke into

the upper troposphere and lower stratosphere where it can be transported across the Northern Hemisphere [*Forster et al.*, 2001; *Turquety et al.*, 2007; *Peterson et al.*, 2018].

Emissions from boreal fires can significantly influence atmospheric composition throughout the Northern Hemisphere. Fire plumes from regional fire complexes in Alaska and western Canada, for example, have been shown to influence air quality over Nova Scotia [*Duck et al.*, 2007] and across the south-central US [*Wotawa et al.*, 2001; *Kasischke et al.*, 2005] and Europe [*Forster et al.*, 2001]. Similarly, fire plumes from Siberia have caused deadly air quality in Moscow [*Konovalov et al..*, 2011] and have affected ozone and other trace gases concentrations across the western US [*Jaffe et al.*, 2004]. Over the past few decades, annual burned area in several regions in boreal North America has increased [*Gillett et al.*, 2004; *Kasischke and Turetsky*, 2006; *Veraverbeke et al.*, 2017], and future projections suggest further increases may occur in response to changes in fire weather and a lengthening of the fire season [*Flannigan et al.*, 2001; *de Groot et al.*, 2013; *Young et al.*, 2017]. As a consequence, fires are likely to play an increasingly important role in regulating air quality and climate feedbacks during the remainder of the 21st century.

To understand boreal fire impacts on the atmosphere, high quality observations characterizing the composition of emissions are necessary [*Andreae and Merlet*, 2001; *Akagi et al.*, 2011]. Here we used trace gas observations from the CARVE (CRV) tower located in interior Alaska (Fox, AK) to derive emission factors of CO and $CH_4$ from boreal forest fires that burned over a period of a month or more during the extreme 2015 fire season. In past work, the most common approach for measuring emission factors from boreal fires is to fly aircraft near or within plumes, measuring trace gases using infrared gas analyzers mounted in the aircraft or by collecting flasks of air that are measured later in the laboratory. A summary of past studies using this technique to measure CO and $CH_4$ emission factors is shown in Table 1. Over a period of more than 25 years, in-situ CO and $CH_4$ emission factors have been measured and reported from a total of 15 boreal fires sampled by aircraft, including 11 wildfires and 4 prescribed fires (Table 1). Additional airborne measurements of trace gas emissions from boreal forest fires are present in the literature, but do not include published CO and/or $CH_4$ emission factors for individual boreal fires. Aircraft sampling is a highly effective approach for sampling large and remote wildfires, especially for characterizing reactive trace gas emissions or aerosols that have lifetimes of hours to days. It also important to recognize potential limits associated with sampling fires in this way. Aircraft observations are mostly confined to periods with good visibility, often sampling well-developed fire plumes during mid-day and during periods with relatively low cloud cover. These environmental conditions represent a subset of the variability that a large wildland fire may experience as it burns over a period of weeks to months. An alternative approach to measuring in-situ emission factors involves using a tower that continuously measures trace gas concentrations located in an area downwind of fires. This has been done in a previous boreal forest fire study during a moderate fire season in Alaska [*Wiggins et al.*, 2016].

Environmental conditions, including weather, vegetation, and edaphic conditions are known to influence the composition of emissions, in part by regulating the importance of flaming and smoldering combustion phases [*Ward and Radke*, 1993; *Yokelson et al.*, 1997; *Akagi et al.*, 2011; *Urbanski*, 2014]. Flaming combustion is more efficient at oxidizing organic matter directly to $CO_2$ gas than smoldering combustion, and as a consequence, smoldering combustion produces more CO, $CH_4$, and organic carbon aerosol [*Ward and Radke*, 1993; *Urbanski et al.*, 2008]. Smoldering combustion can be defined as combustion with a degree of combustion completeness, or modified combustion efficiency, less than 0.9 [*Urbanski*, 2014]. Flaming combustion requires the presence of organic material that burns efficiently in a high oxygen environment [*Ryan et al.,* 2002], and often occurs in boreal forests when fires consume dry aboveground fuels, including vegetation components with low moisture content, litter, and fine woody debris [*French et al.*, 2004]. Smoldering, in contrast, is a dominant combustion phase for burning of belowground biomass and larger coarse woody debris. Residual smoldering combustion in boreal forests can continue to occur for weeks after a flaming fire front has passed through, especially in peatland areas with carbon rich organic soils [*Bertschi et al.*, 2003; *Turquety et al.*,

2007]. Over the lifetime of a large fire, smoldering combustion is more likely to occur during periods with lower temperatures and higher atmospheric humidity that increases the moisture content of fine fuels [*Stocks et al.*, 2001; *Ryan*, 2002].

Here we used trace gas observations of CO, $CH_4$, and $CO_2$ from the CRV tower to estimate emission factors from boreal forest fires that burned during the near-record high Alaska fire season of 2015. The summer of 2015 was the second largest fire

5    season in terms of burned area since records began in 1940 with about 2.1 million hectares burned [*Hayasaka et al.*, 2016; *Partain et al.*, 2016]. An unseasonably warm spring and earlier snowmelt allowed fuels to dry early in the season [*Partain et al.*, 2016]. In mid-June, thunderstorms caused an unprecedented number of lightning strikes (over 65,000) that ignited over 270 individual fires on anomalously dry fuel beds over the course of a week [*Hayasaka et al.*, 2016; *Veraverbeke et al.*, 2017]. Fires expanded dramatically under favorable weather conditions through mid-July, until multiple precipitation events and cool, damp weather

10    minimized fire growth for the rest of the summer fire season.

The CRV tower captured an integrated signal of trace gas emissions from fires across interior Alaska during the 2015 fire season [*Karion et al.*, 2016]. The data stream was comprised of continuous sampling from June 15 – August 15 with more than 65,000 30s averaged samples. The CRV tower experienced enhanced and highly correlated CO, $CH_4$, and $CO_2$ trace gas signals from fires for about 7% of the duration of the 2015 fire season. We identified events when fire emissions had a dominant influence

15    on trace gas variability at CRV tower and used these events to derive emission factors. This data stream represents an order of magnitude increase in sampling density compared with the sum of observations from past work.

We coupled a fire emissions inventory, the Alaska Fire Emissions Database (AKFED) [*Veraverbeke et al.*, 2015] with an atmospheric transport model, the Polar Weather Research and Forecasting Stochastic-Time Integrated Lagrangian Transport (PWRF-STILT) model [*Henderson et al.*, 2015], to quantify the spatial and temporal variability of individual fires and their

20    influence on CO, $CH_4$, and $CO_2$ at the CRV tower. Our tower-based approach allows for an integration of emission factors through the day-night fire cycle and over the full duration of many individual fires. Our results suggest the smoldering phase of boreal fires may have a higher contribution to emissions than previous estimates.

## 2 Methods

### 2.1 CARVE (CRV) Tower Observations

25    Atmospheric CO, $CH_4$, and $CO_2$ mole fractions were measured using a cavity ring-down spectrometer (CRDS, Picarro models 2401 and 2401m) [*Karion et al.*, 2016] at the CRV tower in Fox, Alaska (64.986°N, 147.598°W, ground elevation 611m above sea level). The tower is located about 20 km northeast of Fairbanks Alaska (Figure 1), within the interior forested lowlands and uplands ecoregion in interior Alaska [*Cooper et al.*, 2006]. There are three separate inlets on CRV tower at different heights above ground level from which the spectrometer draws sample air. The spectrometer samples air from the highest level for 50

30    minutes out of every hour, and then draws air from the other levels for 5 minutes at each level [*Karion et al.,* 2016]. The data stream from this spectrometer has gaps every 50 minutes as the spectrometer cycles to the lower inlets. We used observations from air drawn from the top intake height at a height of 32 m above ground level because this level had the highest measurement density and the smallest sensitivity to local ecosystem $CO_2$ fluxes near the tower [*Karion et al.*, 2016]. All raw 30 s average measurements were calibrated according to *Karion et al.* [2016]. Each 30 s average measurement served as an individual point in our calculation

35    of emission factors described below.

### 2.2 Emission Factors and Modified Combustion Efficiency

We isolated intervals when fire had a dominant influence on trace gas variability observed at CRV tower to calculate emission factors. An interval with dominant fire influence was defined as a continuous period that had: 1) a minimum of at least thirty trace gas measurements (with each measurement representing a mean over 30 seconds), 2) a mean CO over the entire interval exceeding 0.5 ppm, and 3) significant correlations between $CO:CO_2$ and $CH_4:CO_2$ exceeding an $r^2$ of 0.80.

5      We used the gaps in the data stream when the spectrometer sampled air from the lower levels to separate the dataset into a set of continuous intervals of trace gas observations with less than 15 s between each new 30 s averaged measurement and by applying a minimum duration criterion of at least 30 measurements. We calculated the mean CO mole fraction for each interval and removed all intervals with a mean CO less than 0.5 ppm. For each interval with high levels of CO, we then extracted CO, $CH_4$, and $CO_2$ mole fractions and calculated correlation coefficients between all three gases. Only periods with high and significant

10    correlations between $CO:CO_2$ and $CH_4:CO_2$ ($r^2 > 0.80$; $p<0.01$, $n > 30$) were retained, because covariance among these co-emitted species is a typical signature of fire emissions [*Urbanski*, 2014].

We calculated background mole fractions of CO and $CH_4$ by taking an average of observations prior to any major fire activity in interior Alaska during DOY 170 – 172.5. This yielded a CO background of 0.110 ppm and a $CH_4$ background of 1.90 ppm. We modeled hourly $CO_2$ background concentrations to account for the influence of net ecosystem exchange (NEE) using a

15    Bayesian approach multi-variable linear regression model trained on CRV tower observations during 2012, a year with little to no fire influence on trace gas variability. We assumed negligible influence from fossil fuel combustion on background mole fractions. The hourly $CO_2$ model was linearly interpolated to have the same temporal resolution as CRV tower data. The variables used in the $CO_2$ model include hourly observations of temperature, vapor pressure deficit, precipitation, day of year, latent heat flux, and hourly $CO_2$ observations from Barrow, AK (Figure 2). Meteorological variables were acquired from the National Climatic Data

20    Center Automated Weather Observing System for Fairbanks International Airport (http://www7.ncdc. noaa.gov/CDO/cdopoemain.cmd). This location was chosen due to its proximity to the CRV tower. We obtained 3-hourly latent heat flux from the NOAH2.7.1 GLDAS/NOAH experiment 001 for version 2 of the Global Land Data Assimilation System (GLDAS-2) [*Rodell et al.*, 2015]. Hourly in-situ $CO_2$ observations from a clean air site in Barrow, AK were attained from the Earth System Research Laboratory Global Monitoring Division [*Thoning et al.*, 2007]. In a sensitivity analysis we found that the removal

25    of the background had only a small effect, because the background did not change appreciably during the duration of each ~50-minute time interval used to compute an emission factor.

We estimated emission ratios ($ER_{CO/CO2}$ and $ER_{CH4/CO2}$) by calculating the slope from a type II linear regression of CO and $CH_4$ excess mole fractions ($\Delta CO$ and $\Delta CH_4$) relative to $CO_2$ ($\Delta CO_2$) (Equation 1). Excess mole fractions refer to observations of trace gas mole fractions during intervals when fire had a dominant influence on tower trace gas variability with background

30    values subtracted. Emission factors ($EF_{CH4/CO2}$ and $EF_{CH4/CO2}$) were calculated by multiplying the emission ratio by a scalar ($S_{CO}$ or $S_{CH4}$) to convert the molar ratio into grams of CO or $CH_4$ emitted per kilogram of dry biomass burned with the assumption that 450 g C is emitted per kilogram of dry biomass consumed ($M_{Biomass}$) [*Yokelson et al.*, 1997; *Akagi et al.*, 2011] (Equation 2).

$$ER_{\frac{CO}{CO_2}} = \frac{\Delta CO}{\Delta CO_2} = \frac{CO_{Fire} - CO_{Background}}{CO_{2\,Fire} - CO_{2\,Background}} \tag{1}$$

$$EF_{\frac{CO}{CO_2}} = ER_{\frac{CO}{CO_2}} * S_{CO} * M_{Biomass} \tag{2}$$

35    We calculated modified combustion efficiency (MCE) for each emission factor period. Modified combustion efficiency is defined as the excess mole fraction of $CO_2$ divided by the sum of the excess mole fractions of CO and $CO_2$ [*Ward and Radke*, 1993]. MCE was used to separate events into three categories: smoldering, mixed, or flaming. These categories reflect the dominant

phase of combustion from fires that contributed to trace gas anomalies at the CRV tower during the summer of 2015. Periods with an MCE less than 0.9 were considered to consist of mostly smoldering combustion, periods with a MCE of greater than or equal to 0.9 and less than 0.92 were classified as consisting of a mixture of smoldering and flaming combustion, and period with an MCE greater than 0.92 were classified as flaming [*Urbanski*, 2014].

5  ## 2.3 Transport Modeling

We coupled a fire emission model, the Alaskan Fire Emissions Database (AKFED) [*Veraverbeke et al.*, 2015] with an atmospheric transport model, the Polar Weather Research and Forecasting Stochastic-Time Integrated Lagrangian Transport model (PWRF-STILT) [*Henderson et al.*, 2015] to estimate fire contribution to trace gas variability from CRV tower observations following *Wiggins et al.* [2016]. AKFED predicts carbon emissions from fires with a temporal resolution of 1 day and a spatial
10  resolution of 450 m. We regridded AKFED to the same spatial resolution as the atmospheric transport model (0.5°) for the model coupling. To account for diurnal variability in emissions, here we imposed a diurnal cycle on daily emissions following *Kaiser et al.* [2009], where the diurnal cycle is the sum of a constant and a Gaussian function that peaks in early afternoon with 90% of emissions occurring during the day (hours 0600 to 1800) and 10% at night (hours 1800 to 0600). PWRF-STILT calculates the sensitivity of atmospheric trace gas measurements to upwind surface fluxes using an influence function or "footprint" [*Henderson*
15  *et al.*, 2015]. The footprints are on a 0.5° latitude-longitude grid with a temporal resolution of 1 h during hours 0600 to 1800 (day) local time and 3 h during hours 1800 to 0600 (night), and provide an estimate of the impact of upwind surface fluxes on CRV tower trace gas measurements at a given time.

We convolved AKFED with the PWRF-STILT footprints to determine individual fire contributions to CO anomalies at CRV tower. This was achieved by calculating the total CO contribution from each individual 0.5° grid cell from the AKFED ×
20  PWRF-STILT combined model and utilizing the fire perimeters from the Alaska Large Fire Database (data provided by Bureau of Land Management (BLM) Alaska Fire Service, on behalf of the Alaska Wildland Fire Coordinating Group (AWFCG) and Alaska Interagency Coordination Center (AICC)) to identify the location of individual fires. AKFED uses the Alaska Large Fire Database for burned area and carbon emissions estimates [*Veraverbeke et al.,* 2015]. We determined an individual fire's contribution to CO at the CRV tower by setting all emissions in AKFED for a particular grid cell to zero and rerunning the model coupling with
25  PWRF-STILT. We confirmed the signals were from a single fire through a complete absence of a modeled enhancement at CRV tower when a specific fire was removed from the simulation. The difference between the original model and the updated coupling is equal to an individual fire's contribution to CO at the CRV tower. Due to the relatively coarse 0.5° grid cell size used for model coupling; more than one fire perimeter existed in some individual grid cells. The contributions for each fire in the same grid cell where determined by weighting the total contribution based on fire size. We also used the influence functions or "footprints" (ppm
30  per μmol/m$^2$/s) from the atmospheric transport model to quantify the contribution of day and night emissions and mean transport times between the point of emission and measurement at the CRV tower. We analyzed the footprints for each time period associated with an emission factor period to confirm CRV tower observations represented an integration of emissions from multiple fires and captured variability in emissions across the diurnal fire cycle.

## 3 Results

35  ### 3.1 Emission Factors and Modified Combustion Efficiency

During the 2015 Alaska fire season, we observed synchronized enhancements of CO, $CH_4$, and $CO_2$ well above background concentrations in CRV tower observations from DOY 173 – 196 (Figure 3). We identified 53 individual events that span about 50 minutes each to calculate emission factors from the elevated trace gas observations (Figure 4; Table 2). $CO/CO_2$ emission ratios ranged from 0.025 to 0.272 and $CH_4/CO_2$ emission ratios ranged from 0.002 to 0.020. MCE ranged from 0.786 to

5    0.975 (Table 2). CO emission factors ranged from 26 to 286 g CO per kg biomass combusted, and $CH_4$ emission factors ranged from 1.21 to 12.2 g $CH_4$ per kg biomass combusted. The mean $CO/CO_2$ emission ratio was $0.138 \pm 0.044$, the mean CO emission factor was $145 \pm 46$ g CO per kg biomass combusted, and the mean MCE was $0.879 \pm 0.068$. Concurrently, the mean $CH_4/CO_2$ emission ratio was $0.010 \pm 0.003$ and the mean $CH_4$ emission factor was $6.05 \pm 1.95$ g $CH_4$ per kg biomass combusted. A strong linear relationship existed between the $CH_4$ emission factor and MCE across the different sampling intervals (Figure 5).

10    Each event was used to calculate emission factors was classified as a smoldering, mixed, or flaming emissions event using the MCE. We categorized 39 smoldering events, 9 mixed events, and 5 flaming events throughout the fire season (examples shown in Figure 6 and Table 3). Smoldering events had a mean $CO/CO_2$ ratio of $0.159 \pm 0.036$, a mean CO emission factor of $167 \pm 38$ g CO per kg biomass combusted, a mean $CH_4/CO_2$ ratio of $0.012 \pm 0.003$, a mean $CH_4$ emission factor of $6.93 \pm 1.59$ g $CH_4$ per kg biomass combusted, and a mean MCE of $0.864 \pm 0.026$. Mixed events consisting of both smoldering and flaming combustion had

15    a mean $CO/CO_2$ emission ratio of $0.096 \pm 0.006$, a mean CO emission factor of $101 \pm 7$ g CO per kg biomass combusted, a mean $CH_4/CO_2$ emission ratio of $0.007 \pm 0.002$, a mean $CH_4$ emission factor of $4.26 \pm 0.95$ g $CH_4$ per kg biomass combusted, and a mean MCE of $0.912 \pm 0.005$. Flaming events had a mean $CO/CO_2$ emission ratio of $0.056 \pm 0.020$, a mean CO emission factor of $58 \pm 21$ g CO per kg biomass combusted, a mean $CH_4/CO_2$ emission ratio of $0.004 \pm 0.001$, a mean $CH_4$ emission factor of $2.49 \pm 0.84$ g $CH_4$ per kg biomass combusted, and a mean MCE of $0.947 \pm 0.018$ (Table 3).

20    **3.2 The Influence of Individual Fires on Trace Gas Variability at the CRV Tower**

The forward model simulations combining AKFED fire emissions with PWRF-STILT confirmed that the elevated CO signals at the CRV tower can be attributed primarily to boreal forest fire emissions (Figure 7). The AKFED model had a Pearson's correlation coefficient of 0.61 with observed daily mean CO and had a low bias of approximately 7%.

We identified 35 individual fires that contributed to at least 1% of the CO mole fraction time series at CRV tower (Figure

25    8; Figure 9; Table 3). On average, these fires were $295 \pm 131$ km away from CRV tower and located mostly to the west of Fairbanks, in the direction of the prevailing summer surface winds. The total CO emitted from these fires accounted for 75% of the excess CO mole fraction signal observed at CRV tower during DOY 160 – 200. The remaining CO signal originated from many smaller fires that were widely distributed across interior Alaska. The Tozitna fire was responsible for the greatest percentage of the total CO anomaly integrated over the 2015 fire season at CRV tower. This fire contributed 11% of the total CO anomaly observed at

30    CRV tower. The fires that significantly contributed the most to the CO anomaly at CRV tower were not necessarily the closest fires to the tower or the largest fires of the 2015 fire season in terms of burned area. Combined, however, this set of 35 fires accounted for 0.97 Mha, or approximately 65% of the total burned area reported during the 2015 fire season [*Veraverbeke et al.*, 2017].

The footprints associated with each emission factor event also were used to determine how much of the signal was coming

35    from burning on previous days and the fraction of emissions emitted during day and night periods. We found that 99% of the fire emissions that influenced CRV tower trace gas concentrations occurred within 3 days of the sampling interval used to derive the emission factor for an individual event at the CRV tower, with 76% occurring within the first 24 hours, 21% during the next 24 hours, and 2% occurring three days prior to the event (Figure 10). Overall, 64% of the fire emissions that impacted the tower occurred during the day (0900 to 1800 local time) and 36% occurred at night (1900 – 0600 local time).

## 4 Discussion

### 4.1 Comparison of tower and aircraft emission factors

Emission factors provide a straightforward way to convert fire emissions of dry biomass into specific trace gas species, such as CO, $CH_4$, and $CO_2$. This technique is commonly used to model emissions of select species and or to compare model results with in-situ or remotely sensed observations. There are limited previous studies on boreal forest fire emission factors, and almost all derived emission factors were determined from aircraft sampling (Table 1) [*Cofer et al.*, 1990; *Radke et al.*, 1991; *Nance et al.*, 1993; *Cofer et al.*, 1998; *Goode et al.*, 2000; *Simpson et al.*, 2011].  In total, all previous aircraft-based studies combined sampled 15 individual prescribed and/or wildfires and derived emission factors that were likely most representative of flaming fires that occurred in the afternoon and were strong enough to generate well-defined plumes. Our emission factors for CO were 35% higher than previous estimates for wildfires derived from the aircraft measurements. We believe a primary contributor to this difference is sampling methodology. Our CRV tower-based sampling was able to integrate over day-night burning cycles, flaming combustion at active fire fronts as well as residual smoldering combustion in soils that persists for days behind the fire line, and emissions associated with a wide range of environmental conditions that occurred during 2015 fire season. This integration was possible because the tower was located several hundred kilometers downwind of the core fire complex located western Alaska. The time delays between emission and detection of trace gas anomalies at CRV allowed for atmospheric mixing of signals from dozens of different fires in different stages of growth and extinction. Collectively, these fires experienced time-varying environmental conditions that were less ideal for flaming combustion than the fire plumes sampled in mid-afternoon by the aircraft.

### 4.2 Integration of emission factor observations across studies and time intervals

Our modeling study confirms that the entire day/night fire cycle was captured by anomalous trace gas observations at CRV tower that was used to calculate emission factors. *Wiggins et al.* [2016] used a similar tower-based approach to estimate boreal forest emission factors during a moderate fire year, and they found CO and $CH_4$ emission factors that were higher than the compiled mean from previous studies. We found a strong linear relationship between $CH_4$ emission factors and MCE that has also been observed in previous studies [*Van Leeuwen and Van Der Werf*, 2011; *Yokelson et al.*, 2013; *Urbanski*, 2014].

Although Table 1 appears to suggest CO emission factors from boreal forest fires are increasing over time, it is more likely that studies using the tower approach are better suited to sample a more thorough representation of all the phases of combustion that can occur in boreal forest fires. The tower approach is not limited by the time or scale of sampling, unlike aircraft measurement techniques. Aircraft based emission factors are often biased towards flaming fires, because most measurements are acquired during the afternoon when active fire plumes are visible. The emission factors derived from this study provide a more robust estimate of the mean, and indicate that the smoldering phase and nighttime emissions of boreal fires have likely been underestimated in previous studies. The improved emission factors from this study can be used in future modeling efforts to convert carbon emissions to CO and $CH_4$ trace gas emissions from boreal forest fires more accurately.

### 4.3 Relative Contributions of Smoldering and Flaming Combustion

Following ignition, boreal forest fires generally begin as stand replacing crown fires followed by smoldering combustion in organic soil layers and coarse woody debris behind the fire front that can continue for weeks after ignition [*Bertschi et al.*, 2003]. This residual smoldering combustion could substantially contribute to trace gas emissions, but is difficult to detect and quantify using remote sensing because of low radiative power associated with this phase of combustion. The relative contributions of

emissions from flaming and smoldering are uncertain for boreal forest fires, but previous studies have assumed 80% of aboveground carbon is consumed in flaming combustion, 20% is consumed in smoldering combustion, and vice versa for belowground carbon [*French et al.*, 2002; *Kasischke and Bruhwiler*, 2002]. Our results suggest that the smoldering phase of combustion contributes to more carbon emissions than has been previously estimated.

### 4.4 Implications of a larger contribution of smoldering combustion

Smoldering combustion produces significantly more CO and $PM_{2.5}$ than flaming combustion [*Bertschi et al.*, 2003; *Chen et al.*, 2007; *Stockwell et al.*, 2016], and corresponding boreal forest fire emissions of these species are likely higher than previous studies suggest. This conclusion implies changes to the overall impact of boreal forest fires on human health, atmospheric composition, and climate. Emissions from boreal forest fires have the potential to be transported long distances across the Northern Hemisphere [*Forster et al.*, 2001], implying large-scale impacts. CO can lead enhanced tropospheric ozone production downwind of a fire [*Lapina et al.*, 2006], and higher concentrations of CO from fires may indirectly contribute to radiative forcing by consuming hydroxyl radicals and extending the lifetime of $CH_4$ [*Levine and Cofer*, 2000]. $PM_{2.5}$ emissions, in contrast, can significantly degrade regional air quality, endanger cardiovascular and respiratory health, and influence the radiative balance of the planet [*Reid et al.*, 2016]. Much of the $PM_{2.5}$ emitted by smoldering fires is composed of organic carbonaceous aerosol that often leads to climate cooling [*Tosca et al.*, 2010; *Jayarathne et al.*, 2018].

### 5 Conclusions

Our tower-based approach to calculate emission factors is a new technique that significantly improves our understanding of trace gas emissions from boreal forest fires. Unlike traditional approaches using aircraft observation, our method represents an integration of trace gas emissions across day and night burning cycles and varying environmental conditions that are both known to considerably influence the composition of fire emissions. We discovered 35 individual fires across interior Alaska significantly influenced trace gas variability at CRV tower from which our emission factors were derived from. This is more than double the number of individual wildfires that have been sampled to calculate boreal fire emission factors in all previous studies combined. Our results suggest the smoldering phase of boreal forest fires contributes to more trace gas emissions than previously believed, and as a consequence, total CO emissions from boreal forest fires may have been underestimated. The tower-based emission factor method introduced in this study can be applied to other biomes and potentially expand in-situ emission factor observations in regions of interest.

### Author Contribution

EBW led the analysis and the writing of the manuscript with contributions from all co-authors. AA, CS, and JBM provided data from the CRV tower. SV provided AKFED data. RC and SW helped define the footprints used in PWRF-STILT. JMH ran the PWRF-STILT model for CRV tower and provided footprints. CEM and JTR contributed to the scientific analysis and the preparation of the manuscript. All authors contributed to the scientific discussion and article preparation.

### Acknowledgements

E.B.W. thanks the U.S. National Science Foundation for a Graduate Research Fellowship (NSF 2013172241). The CRV tower observations and footprints used in our analysis are archived at the U.S. Oak Ridge National Laboratory Distributed Active Archive Center for Biogeochemical Dynamics (http://dx.doi.org/10.3334/ORNLDAAC/1316). The trace gas observations, fire emissions time series, and WRF-STILT model were created through funding support to NASA's CARVE field program led by C. Miller.
5  JTR acknowledges additional NASA support from CMS (80NSSC18K0179), IDS (80NSSC17K0416), and SMAP (NNX16AQ23G) programs. We thank the staff of the NOAA Fairbanks Command and Data Acquisition Station that hosts CRV, and especially Frank Holan and Marc Meindl, for their technical support. We also thank NOAA/ESRL/GMD staff, especially Phil Handley, Jon Kofler, and Tim Newberger for ongoing remote maintenance of CRV.

## References

10  Akagi, S. K., Yokelson, R. J., Wiedinmyer, C., Alvarado, M. J., Reid, J. S., Karl, T., Crounse, J. D. and Wennberg, P. O.: Emission factors for open and domestic biomass burning for use in atmospheric models, Atmos. Chem. Phys., 11, 4039-4072, doi:10.5194/acp-11-4039-2011, 2011.

Andreae, M. O. and Merlet, P.: Emission of trace gases and aerosols from biomass burning, Global Biogeochem. Cycles, 15, 955-966, doi:10.1029/2000GB001382, 2001.

Apps, M. J., Kurz, W. A., Luxmoore, R. J., Nilsson, L. O., Sedjo, R. A., Schmidt, R., Simpson, L. G. and Vinson, T. S.: Boreal forests and tundra, Water, Air, Soil Pollut., 70, 39-43, doi:10.1007/BF01104987, 1993.

20  Bertschi, I., Yokelson, R. J., Ward, D. E., Babbitt, R. E., Susott, R. A., Goode, J. G. and Hao, W. M.: Trace gas and particle emissions from fires in large diameter and belowground biomass fuels, J. Geophys. Res. Atmos., 108, 8472, doi:10.1029/2002JD002100, 2003.

Boby, L. A., Schuur, E. A. G., Mack, M. C., Verbyla, D. and Johnstone, J. F.: Quantifying fire severity, carbon, and nitrogen
25  emissions in Alaska's boreal forest, Ecol. Appl., 20, 1633-1647, doi:10.1890/08-2295.1, 2010.

Chen, L. W. A., Moosmüller, H., Arnott, W. P., Chow, J. C., Watson, J. G., Susott, R. A., Babbitt, R. E., Wold, C. E., Lincoln, E. N. and Wei, M. H.: Emissions from laboratory combustion of wildland fuels: Emission factors and source profiles, Environ. Sci. Technol., 41, 4317-4325, doi:10.1021/es062364i, 2007.
30
Cofer, W. R., Levine, J. S., Winstead, E. L. and Stocks, B. J.: Gaseous emissions from Canadian boreal forest fires, Atmos. Environ. Part A, Gen. Top., 24, 1653-1659, doi:10.1016/0960-1686(90)90499-D, 1990.

Cofer, W. R., Winstead, E. L., Stocks, B. J., Goldammer, J. G. and Cahoon, D. R.: Crown fire emissions of $CO_2$, CO, $H_2$, $CH_4$, and
35  TNMHC from a dense jack pine boreal forest fire, Geophys. Res. Lett., 25, 3919-3922, doi:10.1029/1998GL900042, 1998.

Cooper, D. J., Gallant, A. L., Binnian, E. F., Omernik, J. M. and Shasby, M. B.: Ecoregions of Alaska, Arct. Alp. Res., 29, 494, doi:10.2307/1551999, 2006.

de Groot, W. J., Flannigan, M. D. and Cantin, A. S.: Climate change impacts on future boreal fire regimes, For. Ecol. Manage., 294, 35-44, doi:10.1016/j.foreco.2012.09.027, 2013.

5   Duck, T. J., Firanski, B. J., Millet, D. B., Goldstein, A. H., Allan, J., Holzinger, R., Worsnop, D. R., White, A. B., Stohl, A., Dickinson, C. S. and van Donkelaar, A.: Transport of forest fire emissions from Alaska and the Yukon Territory to Nova Scotia during summer 2004, J. Geophys. Res. Atmos., 112, D10S44, doi:10.1029/2006JD007716, 2007.

Flannigan, M., Campbell, I., Wotton, M., Carcaillet, C., Richard, P. and Bergeron, Y.: Future fire in Canada's boreal forest:
10  paleoecology results and general circulation model - regional climate model simulations, Can. J. For. Res., 31, 854-864, doi:10.1139/x01-010, 2011.

Forster, C., Wandinger, U., Wotawa, G., James, P., Mattis, I., Althausen, D., Simmonds, P., O'Doherty, S., Jennings, S. G., Kleefeld, C., Schneider, J., Trickl, T., Kreipl, S., Jäger, H. and Stohl, A.: Transport of boreal forest fire emissions from Canada to
15  Europe, J. Geophys. Res. Atmos., 106, 22887-22906, doi:10.1029/2001JD900115, 2001.

French, N. H. F., Kasischke, E. S. and Williams, D. G.: Variability in the emission of carbon-based trace gases from wildfire in the Alaskan boreal forest, J. Geophys. Res. Atmos., 107, 8151, doi:10.1029/2001jd000480, 2002.

20  French, N. H. F., Goovaerts, P. and Kasischke, E. S.: Uncertainty in estimating carbon emissions from boreal forest fires, J. Geophys. Res. Atmos., 109, D14S08, doi:10.1029/2003JD003635, 2004.

Gillett, N. P., Weaver, A. J., Zwiers, F. W. and Flannigan, M. D.: Detecting the effect of climate change on Canadian forest fires, Geophys. Res. Lett., 31, L18211, doi:10.1029/2004GL020876, 2004.

Goode, J. G., Yokelson, R. J., Ward, D. E., Susott, R. A., Babbitt, R. E., Davies, M. A. and Hao, W. M.: Measurements of excess $O_3$, $CO_2$, CO, $CH_4$, $C_2H_4$, $C_2H_2$, HCN, NO, $NH_3$, HCOOH, $CH_3COOH$, HCHO, and $CH_3OH$ in 1997 Alaskan biomass burning plumes by airborne Fourier transform infrared spectroscopy (AFTIR), J. Geophys. Res. Atmos., 105, 22147-22166, doi:10.1029/2000jd900287, 2004.

30  Harden, J. W., Trumbore, S. E., Stocks, B. J., Hirsch, A., Gower, S. T., O'Neill, K. P. and Kasischke, E. S.: The role of fire in the boreal carbon budget, Glob. Chang. Biol., 6, 174-184, doi:10.1046/j.1365-2486.2000.06019.x, 2000.

Hayasaka, H., H. L. Tanaka, H. L., and Bieniek, P. A.: Synoptic-scale fire weather conditions in Alaska, Polar Science, 10, 217-226, doi:10.1016/j.polar.2016.05.001, 2016.

35  Henderson, J. M., Eluszkiewicz, J., Mountain, M. E., Nehrkorn, T., Chang, R. Y. W., Karion, A., Miller, J. B., Sweeney, C., Steiner, N., Wofsy, S. C. and Miller, C. E.: Atmospheric transport simulations in support of the Carbon in Arctic Reservoirs Vulnerability Experiment (CARVE), Atmos. Chem. Phys., 15, 4093-4116, doi:10.5194/acp-15-4093-2015, 2015.

Jaffe, D., Bertschi, I., Jaeglé, L., Novelli, P., Reid, J. S., Tanimoto, H., Vingarzan, R. and Westphal, D. L.: Long-range transport of Siberian biomass burning emissions and impact on surface ozone in western North America, Geophys. Res. Lett., 31, L16106, doi:10.1029/2004GL020093, 2004.

5    Jayarathne, T., Stockwell, C.E., Gilbert, A.A., Daugherty, K., Cochrane, M.A., Ryan, K.C., Putra, E.I., Saharjo, B.H., Nurhayati, A.D., Albar, I. and Yokelson, R.J.: Chemical characterization of fine particulate matter emitted by peat fires in Central Kalimantan, Indonesia, during the 2015 El Niño, Atmos. Chem. Phys., 18, 2585-2600, https://doi.org/10.5194/acp-18-2585-2018, 2018.

Johnson, E. A.: Fire and vegetation dynamics: studies from the North American boreal forest, Cambridge University Press, New York, USA, 1996.

Kaiser, J., Suttie, M., Flemming, J., Morcrette, J. J., Boucher, O., and Schultz, M.: Global real-time fire emission estimates based
10   on space-borne fire radiative power observations, in: AIP conference proceedings, 1100, 645, 2009.

Karion, A., Sweeney, C., B Miller, J., E Andrews, A., Commane, R., Dinardo, S., M Henderson, J., Lindaas, J., C Lin, J., A Luus, K., Newberger, T., Tans, P., C Wofsy, S., Wolter, S. and E Miller, C.: Investigating Alaskan methane and carbon dioxide fluxes using measurements from the CARVE tower, Atmos. Chem. Phys., 16, 5383-5398, doi:10.5194/acp-16-5383-2016, 2016.

15   Kasischke, E. S. and Bruhwiler, L. P.: Emissions of carbon dioxide, carbon monoxide, and methane from boreal forest fires in 1998, J. Geophys. Res. Atmos., 107, 8146, doi:10.1029/2001jd000461, 2002.

Kasischke, E. S. and Turetsky, M. R.: Recent changes in the fire regime across the North American boreal region - Spatial and temporal patterns of burning across Canada and Alaska, Geophys. Res. Lett., 33, L09703, doi:10.1029/2006GL025677, 2006.

Kasischke, E. S., Hyer, E. J., Novelli, P. C., Bruhwiler, L. P., French, N. H. F., Sukhinin, A. I., Hewson, J. H. and Stocks, B. J.: Influences of boreal fire emissions on Northern Hemisphere atmospheric carbon and carbon monoxide, Global Biogeochem. Cycles, 19, GB1012, doi:10.1029/2004GB002300, 2005.

25   Konovalov, I. B., Beekmann, M., Kuznetsova, I. N., Yurova, A. and Zvyagintsev, A. M.: Atmospheric impacts of the 2010 Russian wildfires: Integrating modelling and measurements of an extreme air pollution episode in the Moscow region, Atmos. Chem. Phys., 11, 10031-10056, doi:10.5194/acp-11-10031-2011, 2011.

Lapina, K., Honrath, R. E., Owen, R. C., Val Martín, M. and Pfister, G.: Evidence of significant large-scale impacts of boreal fires
30   on ozone levels in the midlatitude Northern Hemisphere free troposphere, Geophys. Res. Lett., 33, L10815, doi:10.1029/2006GL025878, 2006.

Levine, J. S., and Cofer, W. R.: Boreal forest fire emissions and the chemistry of the atmosphere, in: Fire, climate change, and carbon cycling in the boreal forest, Springer, New York, NY, USA,  138, 31-48, https://doi.org/10.1007/978-0-387-21629-4_3,
35   2000.

McGuire, A. D., Macdonald, R. W., Schuur, E. A. G., Harden, J. W., Kuhry, P., Hayes, D. J., Christensen, T. R. and Heimann, M.: The carbon budget of the northern cryosphere region, Curr. Opin. Environ. Sustain., 2, 231-236, doi:10.1016/j.cosust.2010.05.003, 2010.

5   Nance, J. D., Hobbs, P. V., Radke, L. F. and Ward, D. E.: Airborne measurements of gases and particles from an Alaskan wildfire, J. Geophys. Res. Atmos., 98, 14873-14882, doi:10.1029/93jd01196, 2008.

Partain, J. L., Alden, S., Bhatt, U. S., Bieniek, P. A., Brettschneider, B. R., Lader, R. T., Olsson, P. Q., Rupp, T. S., Strader, H., Thoman, R. L., Walsh, J. E., York, A. D. and Ziel, R. H.: 4. An assessment of the role of anthropogenic climate change in the

10   Alaska fire season of 2015, Bull. Am. Meteorol. Soc., 97, S14-S18, doi:10.1175/BAMS-D-16-0149.1, 2016.

Peterson, D. A., Campbell, J. R., Hyer, E. J., Fromm, M. D., Kablick, G. P., Cossuth, J. H. and DeLand, M. T.: Wildfire-driven thunderstorms cause a volcano-like stratospheric injection of smoke, Clim. Atmos. Sci., 1, 30, doi:10.1038/s41612-018-0039-3, 2018.

Radke, L. F., Hegg, D. A., Hobbs, P. V, Nance, J. D., Lyons, J. H., Laursen, K. K., Weiss, R. E., Riggan, P. J. and Ward, D. E.: Particulate and Trace Gas Emissions from Large Biomass Fires in North America, Glob. Biomass Burn. Atmos. Clim. Biosph. Implic., 209-224, 1991.

20   Reid, C. E., Brauer, M., Johnston, F. H., Jerrett, M., Balmes, J. R. and Elliott, C. T.: Critical review of health impacts of wildfire smoke exposure, Environ. Health Perspect., 124, 1334-1343, doi:10.1289/ehp.1409277, 2016.

Rodell, M., Beaudoing, H., and NASA/GSFC/HSL GLDAS Noah Land Surface Model L4 3 hourly 0.25 x 0.25 degree V2. 0, edited, Goddard Earth Sciences Data and Information Services Center (GES DISC) Greenbelt, MD, 2015.

25   Rogers, B. M., Soja, A. J., Goulden, M. L. and Randerson, J. T.: Influence of tree species on continental differences in boreal fires and climate feedbacks, Nat. Geosci., 8, 228-234, doi:10.1038/ngeo2352, 2015.

Ryan, K. C.: Dynamic interactions between forest structure and fire behavior in boreal ecosystems, in Silva Fennica., 36, 13-39, 2002.

30

Simpson, I. J., Akagi, S. K., Barletta, B., Blake, N. J., Choi, Y., Diskin, G. S., Fried, A., Fuelberg, H. E., Meinardi, S., Rowland, F. S., Vay, S. A., Weinheimer, A. J., Wennberg, P. O., Wiebring, P., Wisthaler, A., Yang, M., Yokelson, R. J. and Blake, D. R.: Boreal forest fire emissions in fresh Canadian smoke plumes: C1-C10 volatile organic compounds (VOCs), $CO_2$, CO, $NO_2$, NO, HCN and $CH_3CN$, Atmos. Chem. Phys., 11, 6445-6463, doi:10.5194/acp-11-6445-2011, 2011.

35

Stocks, B., Wotton, B., Flannigan, M., Fosberg, M., Cahoon, D., and Goldammer, J.: Boreal forest fire regimes and climate change, in: Remote sensing and climate modeling: Synergies and limitations, edited by: Beniston, M., and Verstraete, M. M., Springer, Dordrecht, 233-246, https://doi.org/10.1007/0-306-48149-9, 2001.

Stockwell, C. E., Jayarathne, T., Cochrane, M.A., Ryan, K. C., Putra, E. I., Saharjo, B. H., Nurhayati, A. D., Albar, I., Blake, D. R., Simpson, I. J. and Stone, E. A.: Field measurements of trace gases and aerosols emitted by peat fires in Central Kalimantan, Indonesia, during the 2015 El Niño, Atmos. Chem. Phys., 16, 11711-11732, doi: 10.5194/acp-16-11711-2016, 2016.

5    Thoning, K., Kitzis, D., and Crotwell, A.: Atmospheric carbon dioxide dry air mole fractions from quasi-continuous measurements at Barrow, Alaska, Mauna Loa, Hawaii, American Samoa, and South Pole, 1973–2006, Version: 2007-10-01, National Oceanic and Atmospheric Administration, Path: ftp://ftp.cmdl.noaa.gov/ccg/co2/in-situ, 2007.

Tosca, M. G., Randerson, J.T., Zender, C.S., Flanner, M.G. and Rasch, P.J.:  Do biomass burning aerosols intensify drought in equatorial Asia during El Niño?, Atmos. Chem. Phys., 10, 3515-3528, https://doi.org/10.5194/acp-10-3515-2010, 2010.

10   Turquety, S., Logan, J. A., Jacob, D. J., Hudman, R. C., Leung, F. Y., Heald, C. L., Yantosca, R. M., Wu, S., Emmons, L. K., Edwards, D. P. and Sachse, G. W.: Inventory of boreal fire emissions for North America in 2004: Importance of peat burning and pyroconvective injection, J. Geophys. Res. Atmos., 112, D12S03, doi:10.1029/2006JD007281, 2007.

Urbanski, S.: Wildland fire emissions, carbon, and climate: Emission factors, For. Ecol. Manage., 317, 51-60,
15   doi:10.1016/j.foreco.2013.05.045, 2014.

Urbanski, S. P., Hao, W. M. and Baker, S.: Chapter 4 Chemical Composition of Wildland Fire Emissions, Dev. Environ. Sci., 8, 79-107, doi:10.1016/S1474-8177(08)00004-1, 2008.

20   Van Leeuwen, T. T. and Van Der Werf, G. R.: Spatial and temporal variability in the ratio of trace gases emitted from biomass burning, Atmos. Chem. Phys., 11, 3611-3629, doi:10.5194/acp-11-3611-2011, 2011.

Veraverbeke, S., Rogers, B. M. and Randerson, J. T.: Daily burned area and carbon emissions from boreal fires in Alaska, Biogeosciences, 12, 3579-3601, doi:10.5194/bg-12-3579-2015, 2015.

Veraverbeke, S., Rogers, B. M., Goulden, M. L., Jandt, R. R., Miller, C. E., Wiggins, E. B. and Randerson, J. T.: Lightning as a major driver of recent large fire years in North American boreal forests, Nat. Clim. Chang., 7, 529-534, doi:10.1038/nclimate3329, 2017.

30   Walker, X. J., Baltzer, J. L., Cumming, S. G., Day, N. J., Johnstone, J. F., Rogers, B. M., Solvik, K., Turetsky, M. R. and Mack, M. C.: Soil organic layer combustion in boreal black spruce and jack pine stands of the Northwest Territories, Canada, Int. J. Wildl. Fire, 27, 125-134, doi:10.1071/wf17095, 2018.

Ward, D. E. and Radke, L. F.: Emissions Measurements from Vegetation Fires: A Comparative Evaluation of Methods and Results,
35   Fire in the Environment: The Ecological Atmospheric and Climatic Importance of Vegetation Fires, 13, 53-76, 1993.

Ward, D. S., Kloster, S., Mahowald, N. M., Rogers, B. M., Randerson, J. T., and Hess, P. G.: The changing radiative forcing of fires: global model estimates for past, present and future, Atmos. Chem. Phys., 12, 10857–10886, 2012.

Wiggins, E. B., Veraverbeke, S., Henderson, J. M., Karion, A., Miller, J. B., Lindaas, J., Commane, R., Sweeney, C., Luus, K. A., Tosca, M. G., Dinardo, S. J., Wofsy, S., Miller, C. E. and Randerson, J. T.: The influence of daily meteorology on boreal fire emissions and regional trace gas variability, J. Geophys. Res. Biogeosciences, 121, 2793-2810, doi:10.1002/2016JG003434, 2016.

5    Wotawa, G., Novelli, P. C., Trainer, M. and Granier, C.: Inter-annual variability of summertime CO concentrations in the Northern Hemisphere explained by boreal forest fires in North America and Russia, Geophys. Res. Lett., 28, 4575-4578, doi:10.1029/2001GL013686, 2001.

Yokelson, R. J., Susott, R., Ward, D. E., Reardon, J. and Griffith, D. W. T.: Emissions from smoldering combustion of biomass
10   measured by open-path Fourier transform infrared spectroscopy, J. Geophys. Res. Atmos., 102, 18865-18877, doi:10.1029/97jd00852, 2004.

Yokelson, R. J., Burling, I. R., Gilman, J. B., Warneke, C., Stockwell, C. E., De Gouw, J., Akagi, S. K., Urbanski, S. P., Veres, P., Roberts, J. M., Kuster, W. C., Reardon, J., Griffith, D. W. T., Johnson, T. J., Hosseini, S., Miller, J. W., Cocker, D. R., Jung, H.
15   and Weise, D. R.: Coupling field and laboratory measurements to estimate the emission factors of identified and unidentified trace gases for prescribed fires, Atmos. Chem. Phys., 13, 89-116, doi:10.5194/acp-13-89-2013, 2013.

Young, A. M., Higuera, P. E., Duffy, P. A. and Hu, F. S.: Climatic thresholds shape northern high-latitude fire regimes and imply vulnerability to future climate change, Ecography, 40, 606-617, doi:10.1111/ecog.02205, 2017.
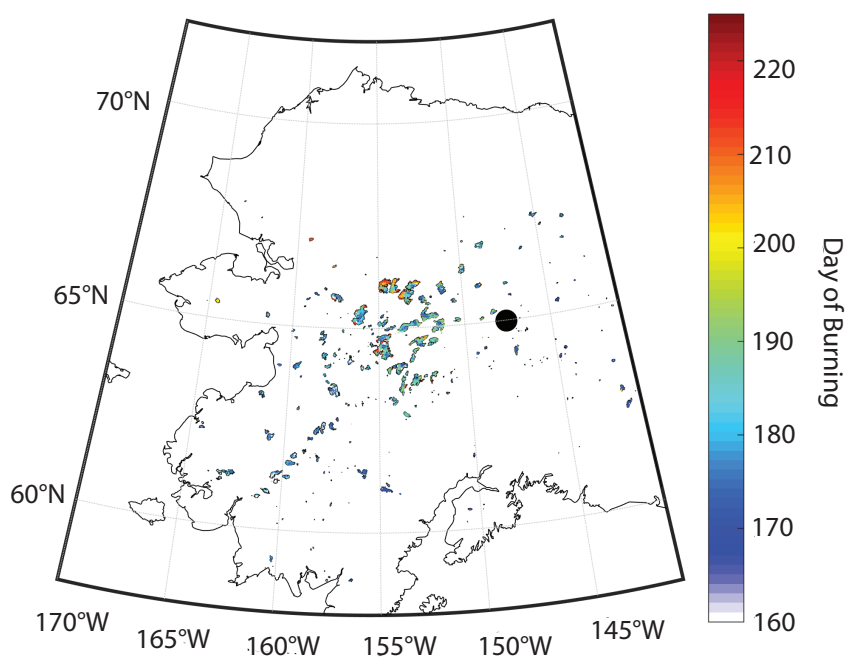
**Figures**

**Figure 1.** Burned area in Alaska during 2015 with colors representing the day of ignition. Black circle denotes the location of CRV tower.
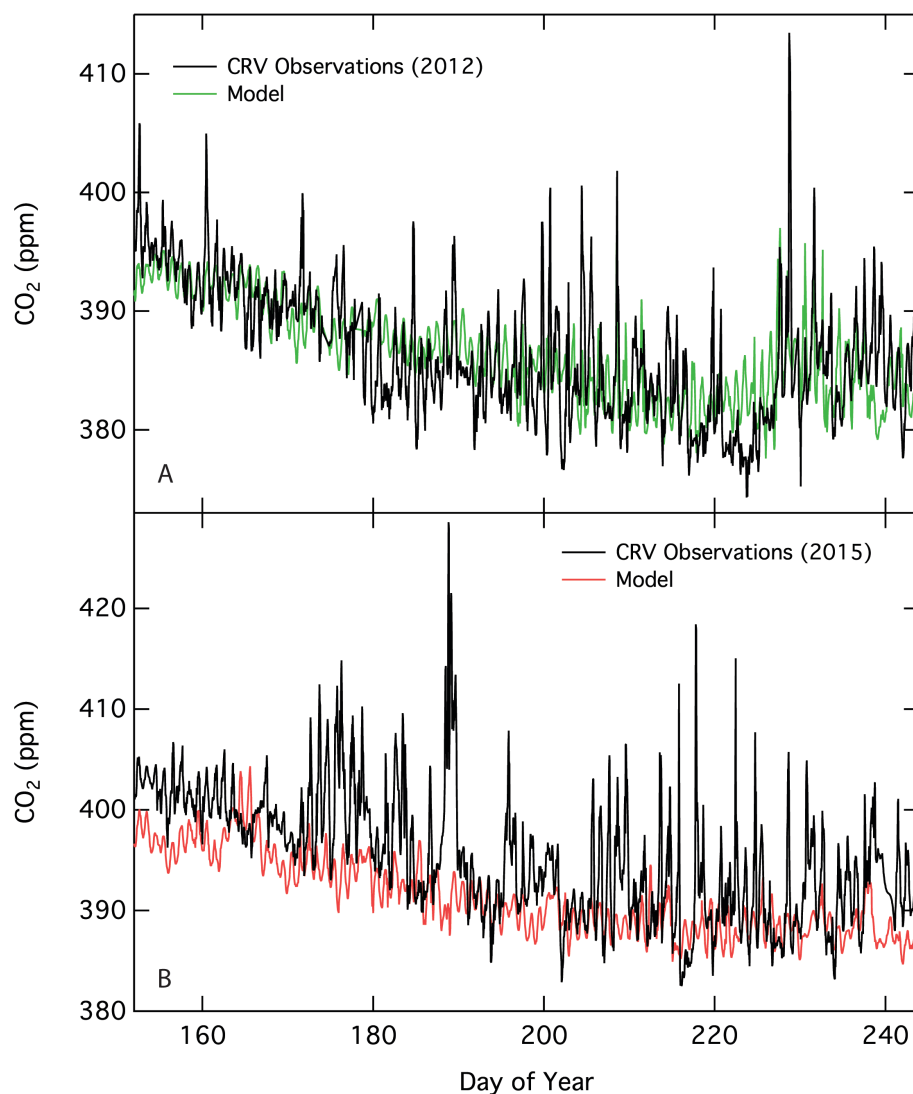
**Figure 2.** Panel A: 2012 $CO_2$ observations from CRV tower (black) during a low fire year versus modeled background $CO_2$ (green). Panel B: 2015 $CO_2$ observations from CRV tower (black) versus modeled background $CO_2$ (red).
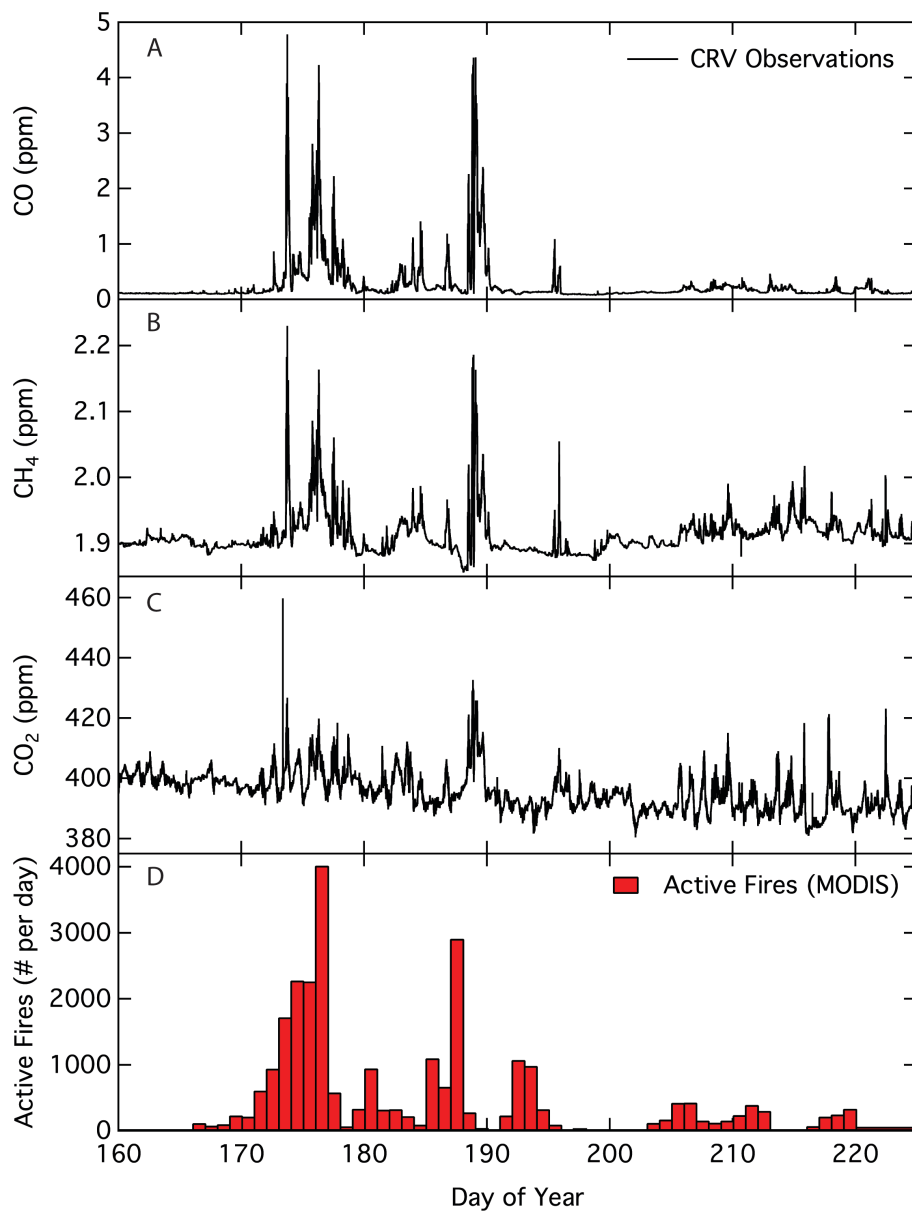
**Figure 3.** Panels A-C: trace gas observations (black) from CRV tower during the summer of 2015. Panel D: number of daily active fires from MODIS (red).
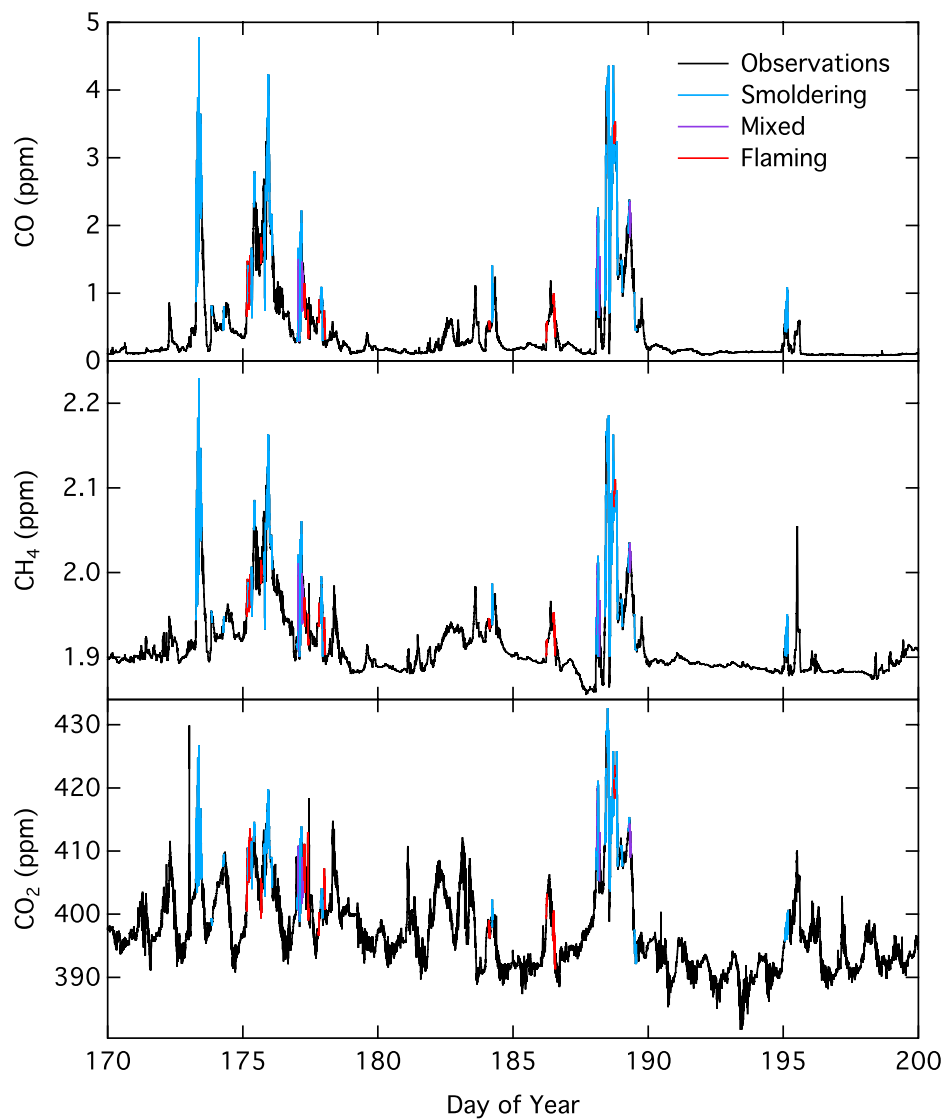
**Figure 4.** CRV tower observations of CO (panel A), $CH_4$ (panel B), and $CO_2$ (panel C) with periods used to calculate emission factors highlighted to denote the dominant phase of combustion - smoldering (blue), mixed (purple), and flaming (red).

**Figure 5.** Relationship between CH₄ emission factors and corresponding modified combustion efficiency (MCE).
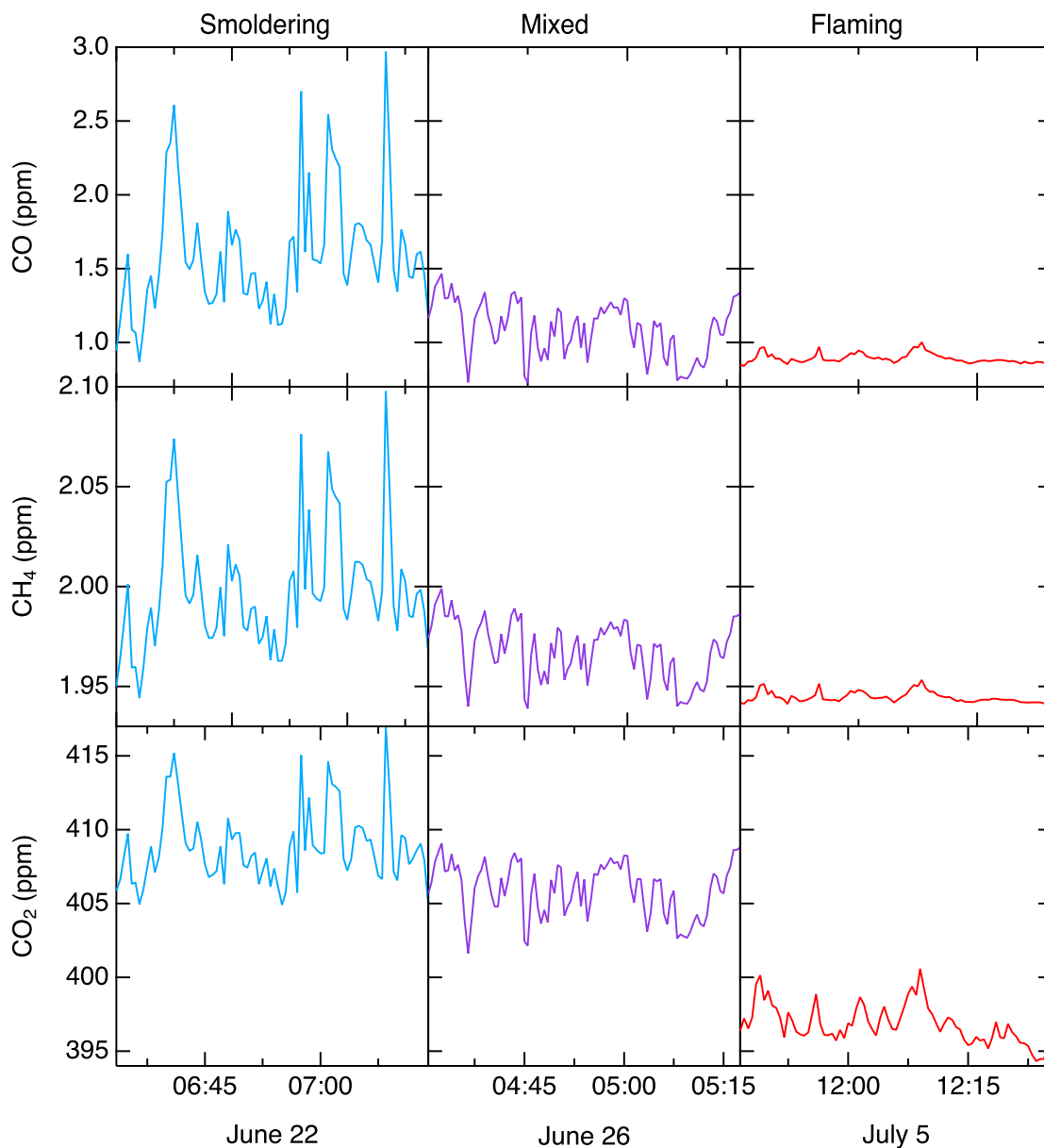
**Figure 6.** Examples of raw trace gas observations used to calculate emission factors for smoldering (blue), mixed (purple), and flaming (red) dominated combustion. All dates are from 2015 and in military time.
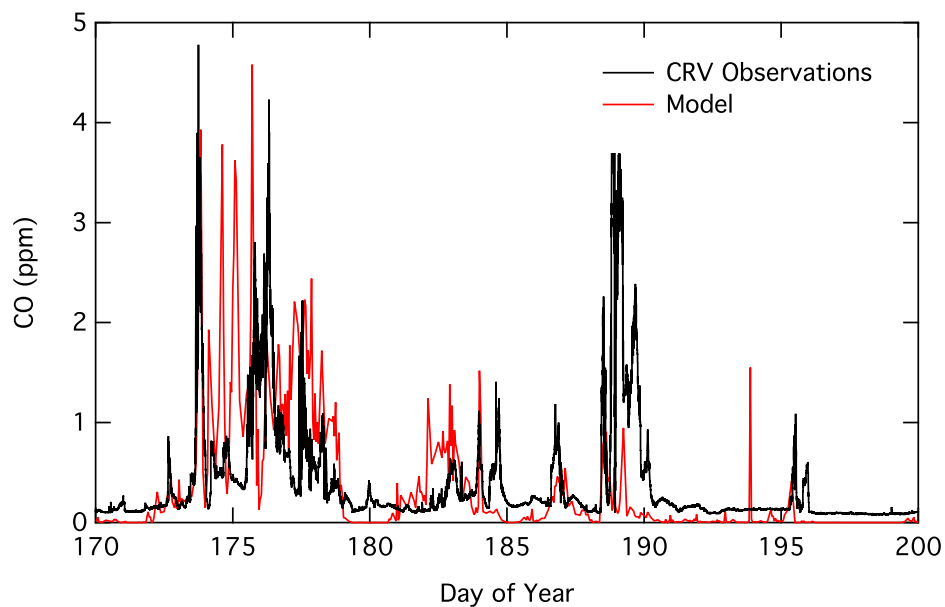
**Figure 7.** CRV observations of CO (black) compared to modeled CO anomaly due to fires (red).
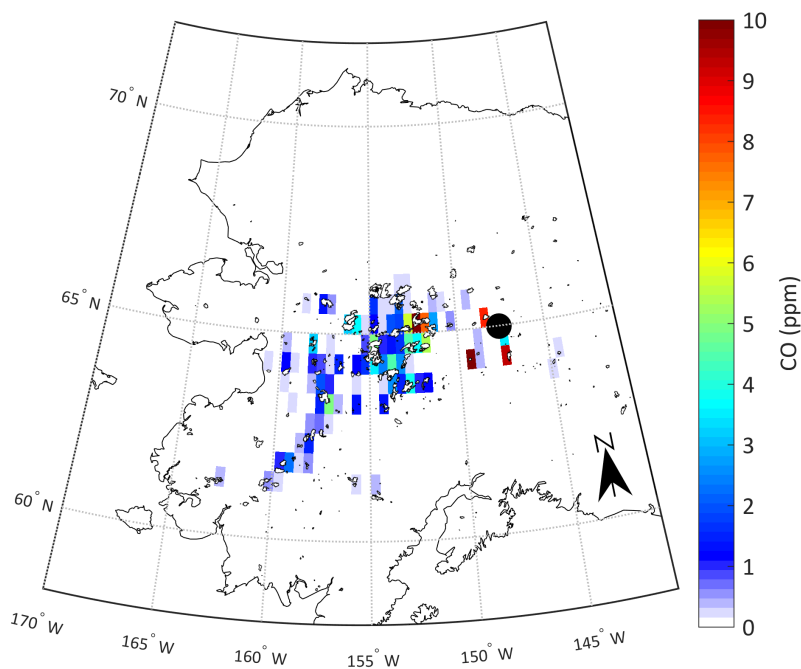
**Figure 8.** Total individual fire contributions to CO anomaly at CRV tower determined by convolving footprints from PWRF-
5   STILT with fire emissions from AKFED. The location of CRV tower is shown as a black dot. Fire perimeters are shown as black
outlines.
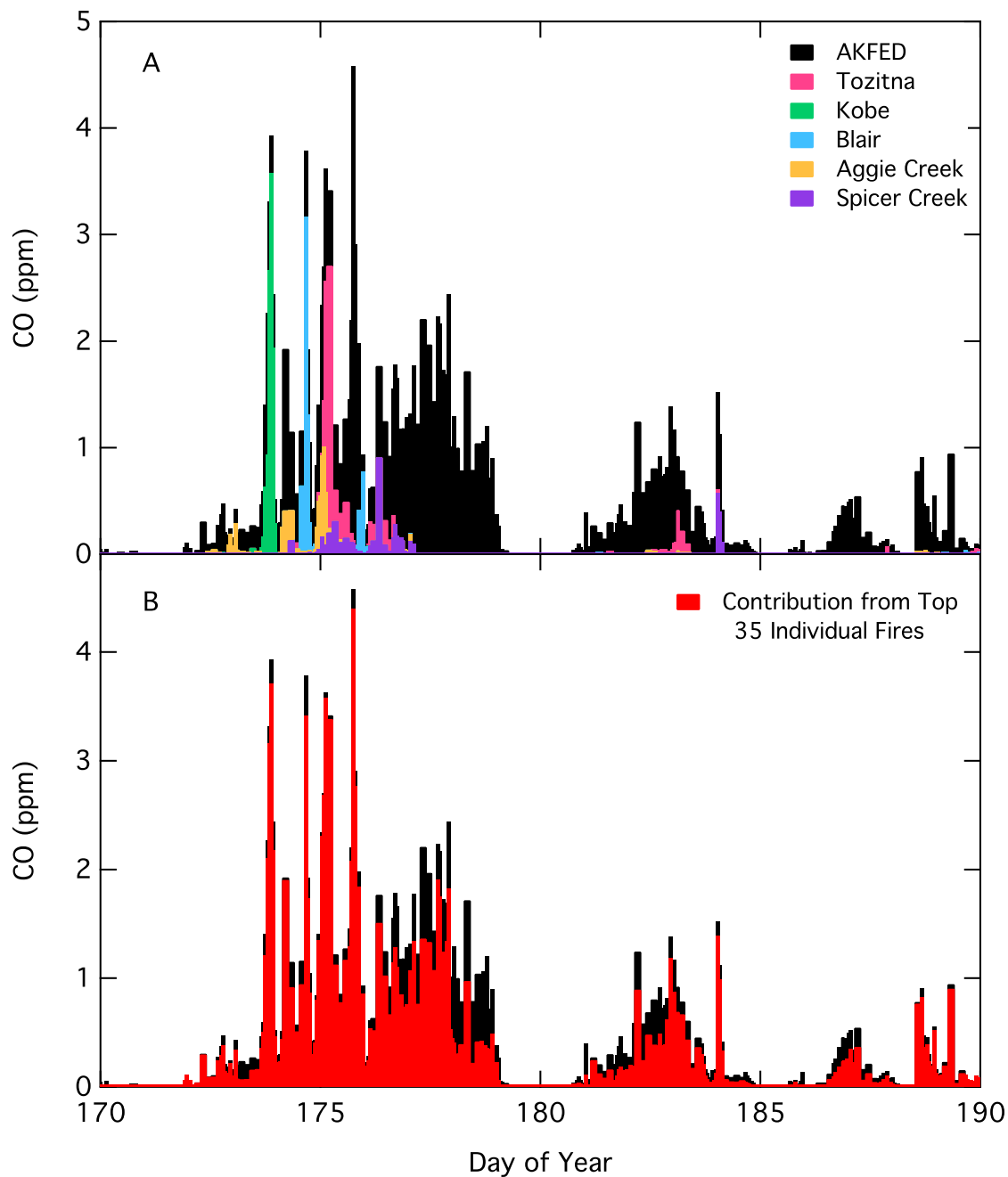
**Figure 9.** A) Largest 5 individual fire contributions to the CO anomaly simulated at CRV tower. Black shows original AKFED ×
PWRF-STILT model, red depicts contributions from the Tozitna fire, green from Kobe fire, blue from Blair fire, gold from Aggie
Creek fire, and purple from Spicer Creek fire. B) The total CO anomaly from all fires that contributed to at least 1% of the modeled
CO anomaly at CRV tower (red) compared to the original model (black).
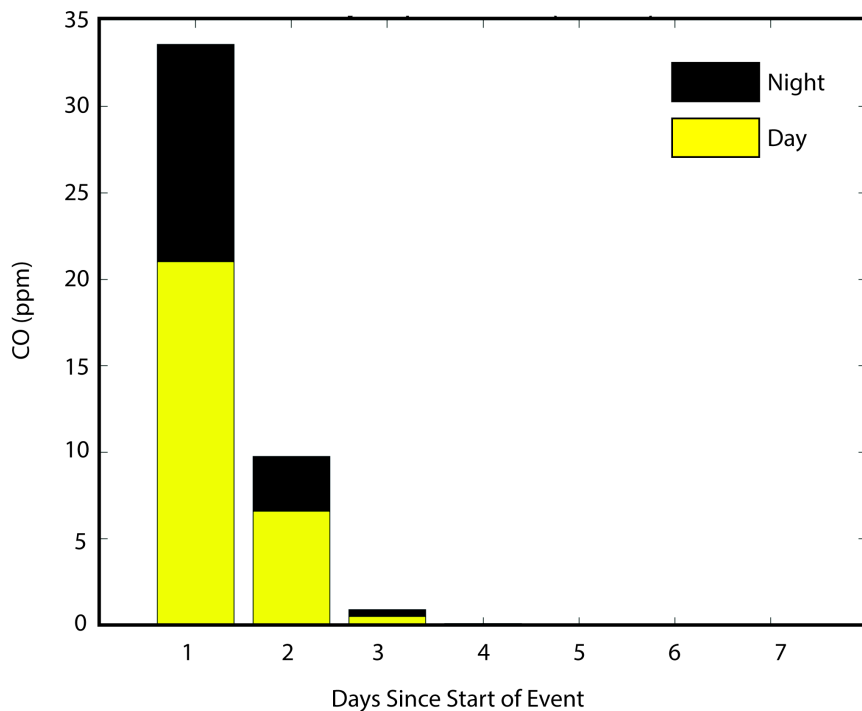
**Figure 10.** Temporal distribution of CO anomaly at the CRV tower caused by fires, calculated by multiplying footprints from PWRF-STILT with fire emissions from AKFED. Only times when emission ratios were calculated are used in the analysis.

**Tables**

| Study | Location | # Fires Sampled | Sampling Strategy | CO Emission Ratio | | | | CO Emission Factor | MCE |
|---|---|---|---|---|---|---|---|---|---|
| | | | | Mean | Flaming | Mixed | Smoldering | | |
| **Prescribed Fires** | | | | | | | | | |
| Cofer et al. (1990) | Canada | 2 | Flask (A) | 0.096 ± 0.010 | 0.064 ± 0.006 | 0.103 ± 0.006 | 0.122 ± 0.018 | 102 ± 29 | 0.912 ± 0.016 |
| Cofer et al. (1998) | Canada | 2 | Flask (A) | 0.140 ± 0.001 | 0.094 ± 0.001 | | 0.185 ± 0.001 | 148 ± 13 | 0.877 ± 0.002 |
| **Wildfires** | | | | | | | | | |
| Radke et al. (1991) | Canada | 1 | Gas Analyzer (A) | 0.095 ± 0.049 | | | | 101 ± 52 | 0.913 ± 0.082 |
| Nance et al. (1993) | Alaska | 1 | Flask (A) | 0.078 ± 0.001 | | | | 83 ± 12 | 0.927 ± 0.002 |
| Goode et al. (2000) | Alaska | 4 | Gas Analyzer (A) | 0.085 ± 0.008 | | | | 90 ± 9 | 0.922 ± 0.014 |
| Simpson et al. (2011) | Canada | 5 | Flasks (A) | 0.110 ± 0.070 | | | | 117 ± 72 | 0.901 ± 0.061 |
| Mean | | 15 | | 0.102 ± 0.030 | 0.079 ± 0.004 | 0.103 ± 0.006 | 0.154 ± 0.010 | 109 ± 36 | 0.907 ± 0.032 |
| This Study | Alaska | 35 | Gas Analyzer (G) | 0.138 ± 0.048 | 0.056 ± 0.020 | 0.096 ± 0.006 | 0.159 ± 0.036 | 145 ± 46 | 0.879 ± 0.068 |

**Table 1**. Comparison of CO and $CH_4$ emission ratios, emission factors, and modified combustion efficiency (MCE) from previous studies that measured in-situ boreal fires. Number of fires sampled per study is given in parenthesis following the location. Aircraft

5 based studies are denoted with an (A) following the sampling strategy and ground based studies are denoted with a (G) following the sampling strategy. The studies are organized based on the type of fire they measured, prescribed fires or wildfires. We did not include studies that measured slash and tramp prescribed fires or laboratory fires. The CO emission ratio column has units of ppmv ppmv$^{-1}$ and use $CO_2$ as the reference gas. This column is separated into the mean per study and by fire combustion phase including flaming, mixed, and smoldering when available. Emission factors were calculated from emission ratios assuming the carbon

10 content of combusted fuel was 45% when not provided by the study. MCE was calculated as 1/(1+CO emission ratio) when not given in the study. The weighted mean of emission ratios, emission factors, and MCE for all previous aircraft based studies is shown in the row labeled mean, with each study weighted by the number of fires sampled.

| Event | N | Time of Event | CO Emission Ratio | CO Emission Factor | CH$_4$ Emission Ratio | CH$_4$ Emission Factor | Modified Combustion Efficiency | Combustion Phase |
|---|---|---|---|---|---|---|---|---|
| 1 | 82 | 173.27 - 173 | 0.161 ± 0.004 | 169 ± 4.32 | 0.012 ± 0.0003 | 7.14 ± 0.16 | 0.861 ± 0.006 | Smoldering |
| 2 | 95 | 173.32 - 173 | 0.151 ± 0.004 | 159 ± 4.15 | 0.011 ± 0.0002 | 6.78 ± 0.15 | 0.869 ± 0.006 | Smoldering |
| 3 | 95 | 173.36 - 173 | 0.141 ± 0.003 | 148 ± 3.10 | 0.010 ± 0.0002 | 6.28 ± 0.13 | 0.877 ± 0.005 | Smoldering |
| 4 | 83 | 173.40 - 173 | 0.149 ± 0.008 | 156 ± 7.94 | 0.011 ± 0.0005 | 6.41 ± 0.32 | 0.870 ± 0.011 | Smoldering |
| 5 | 95 | 173.45 - 173 | 0.130 ± 0.006 | 137 ± 5.97 | 0.009 ± 0.0004 | 5.64 ± 0.25 | 0.885 ± 0.009 | Smoldering |
| 6 | 95 | 173.84 - 173 | 0.136 ± 0.008 | 143 ± 8.01 | 0.014 ± 0.0009 | 8.40 ± 0.52 | 0.880 ± 0.012 | Smoldering |
| 7 | 85 | 174.27 - 174 | 0.170 ± 0.008 | 178 ± 8.13 | 0.008 ± 0.0003 | 5.08 ± 0.20 | 0.855 ± 0.011 | Smoldering |
| 8 | 95 | 175.15 - 175 | 0.080 ± 3e-4 | 84 ± 0.33 | 0.004 ± 3e-5 | 2.51 ± 0.02 | 0.926 ± 0.001 | Flaming |
| 9 | 95 | 175.19 - 175 | 0.143 ± 0.007 | 151 ± 7.25 | 0.008 ± 0.0004 | 4.83 ± 0.25 | 0.875 ± 0.011 | Smoldering |
| 10 | 58 | 175.23 - 175 | 0.091 ± 0.002 | 96 ± 2.20 | 0.005 ± 0.0002 | 2.78 ± 0.11 | 0.916 ± 0.004 | Mixed |
| 11 | 88 | 175.27 - 175 | 0.091 ± 0.001 | 96 ± 1.43 | 0.005 ± 0.0001 | 3.15 ± 0.04 | 0.917 ± 0.002 | Mixed |
| 12 | 95 | 175.32 - 175 | 0.153 ± 0.003 | 161 ± 3.51 | 0.009 ± 0.0002 | 5.19 ± 0.10 | 0.867 ± 0.005 | Smoldering |
| 13 | 89 | 175.40 - 175 | 0.187 ± 0.012 | 196 ± 12.3 | 0.013 ± 0.0008 | 7.73 ± 0.48 | 0.842 ± 0.017 | Smoldering |
| 14 | 95 | 175.66 - 175 | 0.060 ± 0.003 | 63 ± 3.05 | 0.005 ± 0.0002 | 2.71 ± 0.12 | 0.943 ± 0.005 | Flaming |
| 15 | 55 | 175.75 - 175 | 0.129 ± 0.001 | 135 ± 1.43 | 0.009 ± 0.0001 | 5.13 ± 0.07 | 0.886 ± 0.002 | Smoldering |
| 16 | 35 | 175.77 - 175 | 0.237 ± 0.015 | 248 ± 15.4 | 0.017 ± 0.0010 | 10.1 ± 0.60 | 0.809 ± 0.019 | Smoldering |
| 17 | 95 | 175.80 - 175 | 0.147 ± 0.002 | 154 ± 2.00 | 0.011 ± 0.0001 | 6.32 ± 0.06 | 0.872 ± 0.003 | Smoldering |
| 18 | 95 | 175.88 - 175 | 0.155 ± 0.003 | 162 ± 3.40 | 0.009 ± 0.0002 | 5.71 ± 0.15 | 0.866 ± 0.005 | Smoldering |
| 19 | 95 | 175.92 - 175 | 0.198 ± 0.004 | 207 ± 4.44 | 0.012 ± 0.0001 | 7.37 ± 0.07 | 0.835 ± 0.006 | Smoldering |
| 20 | 80 | 175.98 - 176 | 0.193 ± 0.003 | 203 ± 2.67 | 0.011 ± 0.0001 | 6.50 ± 0.09 | 0.838 ± 0.004 | Smoldering |
| 21 | 95 | 176.06 - 176 | 0.119 ± 0.007 | 125 ± 7.49 | 0.008 ± 0.0004 | 5.00 ± 0.27 | 0.893 ± 0.011 | Smoldering |
| 22 | 95 | 177.06 - 177 | 0.105 ± 0.001 | 110 ± 1.01 | 0.010 ± 0.0001 | 5.77 ± 0.04 | 0.905 ± 0.002 | Mixed |
| 23 | 75 | 177.11 - 177 | 0.122 ± 0.002 | 128 ± 2.10 | 0.011 ± 0.0001 | 6.34 ± 0.09 | 0.892 ± 0.003 | Smoldering |
| 24 | 95 | 177.15 - 177 | 0.129 ± 0.001 | 135 ± 1.41 | 0.010 ± 0.0001 | 6.28 ± 0.07 | 0.886 ± 0.002 | Smoldering |
| 25 | 95 | 177.19 - 177 | 0.102 ± 0.002 | 107 ± 2.31 | 0.008 ± 0.0002 | 4.87 ± 0.11 | 0.908 ± 0.004 | Mixed |
| 26 | 58 | 177.23 - 177 | 0.148 ± 0.011 | 155 ± 11.6 | 0.012 ± 0.0009 | 6.94 ± 0.53 | 0.871 ± 0.017 | Smoldering |
| 27 | 94 | 177.27 - 177 | 0.060 ± 0.002 | 63 ± 1.61 | 0.004 ± 0.0001 | 2.47 ± 0.06 | 0.944 ± 0.003 | Flaming |
| 28 | 95 | 177.80 - 177 | 0.094 ± 0.002 | 98 ± 2.10 | 0.008 ± 0.0001 | 4.52 ± 0.09 | 0.914 ± 0.003 | Mixed |
| 29 | 95 | 177.88 - 177 | 0.120 ± 0.006 | 126 ± 5.99 | 0.020 ± 0.0012 | 12.2 ± 0.71 | 0.893 ± 0.009 | Smoldering |
| 30 | 95 | 177.92 - 177 | 0.161 ± 0.006 | 169 ± 5.94 | 0.017 ± 0.0007 | 10.3 ± 0.39 | 0.861 ± 0.008 | Smoldering |
| 31 | 95 | 183.62 - 183 | 0.114 ± 0.004 | 120 ± 4.47 | 0.009 ± 0.0003 | 5.58 ± 0.20 | 0.897 ± 0.007 | Smoldering |
| 32 | 95 | 184.23 - 184 | 0.232 ± 0.014 | 244 ± 14.9 | 0.013 ± 0.0007 | 8.06 ± 0.43 | 0.811 ± 0.019 | Smoldering |
| 33 | 80 | 186.49 - 186 | 0.025 ± 0.002 | 26 ± 1.77 | 0.002 ± 0.0001 | 1.21 ± 0.07 | 0.976 ± 0.003 | Flaming |
| 34 | 95 | 188.06 - 188 | 0.190 ± 0.002 | 200 ± 2.62 | 0.013 ± 0.0002 | 8.12 ± 0.10 | 0.840 ± 0.004 | Smoldering |
| 35 | 95 | 188.10 - 188 | 0.106 ± 0.002 | 111 ± 2.28 | 0.008 ± 0.0002 | 5.00 ± 0.10 | 0.904 ± 0.004 | Mixed |
| 36 | 95 | 188.14 - 188 | 0.115 ± 0.001 | 120 ± 1.12 | 0.008 ± 0.0001 | 5.03 ± 0.04 | 0.897 ± 0.002 | Smoldering |
| 37 | 85 | 188.19 - 188 | 0.097 ± 0.002 | 102 ± 2.11 | 0.007 ± 0.0002 | 4.34 ± 0.09 | 0.911 ± 0.003 | Mixed |
| 38 | 95 | 188.40 - 188 | 0.194 ± 0.003 | 204 ± 2.64 | 0.012 ± 0.0002 | 7.34 ± 0.09 | 0.837 ± 0.004 | Smoldering |
| 39 | 95 | 188.45 - 188 | 0.131 ± 0.004 | 138 ± 3.89 | 0.013 ± 0.0006 | 7.89 ± 0.34 | 0.884 ± 0.006 | Smoldering |
| 40 | 36 | 188.53 - 188 | 0.146 ± 0.002 | 153 ± 1.71 | 0.012 ± 0.0001 | 6.95 ± 0.05 | 0.873 ± 0.002 | Smoldering |
| 41 | 95 | 188.58 - 188 | 0.158 ± 0.001 | 166 ± 1.00 | 0.012 ± 0.0001 | 7.25 ± 0.04 | 0.863 ± 0.001 | Smoldering |
| 42 | 95 | 188.62 - 188 | 0.179 ± 0.002 | 188 ± 2.06 | 0.014 ± 0.0002 | 8.21 ± 0.10 | 0.848 ± 0.003 | Smoldering |
| 43 | 74 | 188.66 - 188 | 0.214 ± 0.011 | 224 ± 11.6 | 0.015 ± 0.0008 | 9.12 ± 0.47 | 0.824 ± 0.015 | Smoldering |
| 44 | 95 | 188.71 - 188 | 0.138 ± 0.005 | 145 ± 4.85 | 0.010 ± 0.0004 | 5.87 ± 0.22 | 0.879 ± 0.007 | Smoldering |
| 45 | 95 | 188.75 - 188 | 0.055 ± 0.003 | 58 ± 3.42 | 0.006 ± 0.0002 | 3.54 ± 0.13 | 0.948 ± 0.006 | Flaming |
| 46 | 95 | 188.79 - 188 | 0.272 ± 0.009 | 286 ± 9.92 | 0.012 ± 0.0005 | 7.29 ± 0.27 | 0.786 ± 0.012 | Smoldering |
| 47 | 52 | 188.84 - 188 | 0.120 ± 0.002 | 126 ± 1.72 | 0.009 ± 0.0001 | 5.52 ± 0.08 | 0.893 ± 0.003 | Smoldering |
| 48 | 39 | 188.86 - 188 | 0.091 ± 0.002 | 96 ± 2.12 | 0.007 ± 0.0001 | 4.39 ± 0.06 | 0.916 ± 0.003 | Mixed |
| 49 | 59 | 189.03 - 189 | 0.154 ± 0.012 | 162 ± 12.6 | 0.010 ± 0.0008 | 6.19 ± 0.47 | 0.867 ± 0.018 | Smoldering |
| 50 | 95 | 189.27 - 189 | 0.149 ± 0.008 | 156 ± 8.88 | 0.011 ± 0.0005 | 6.43 ± 0.33 | 0.871 ± 0.013 | Smoldering |
| 51 | 30 | 189.34 - 189 | 0.090 ± 0.009 | 95 ± 9.46 | 0.006 ± 0.0005 | 3.54 ± 0.32 | 0.917 ± 0.015 | Mixed |
| 52 | 89 | 189.49 - 189 | 0.165 ± 0.009 | 173 ± 9.44 | 0.012 ± 0.0007 | 7.19 ± 0.39 | 0.858 ± 0.013 | Smoldering |
| 53 | 95 | 195.14 - 195 | 0.140 ± 0.007 | 147 ± 7.61 | 0.010 ± 0.0006 | 6.31 ± 0.33 | 0.877 ± 0.011 | Smoldering |
| Mean | | | 0.138 ± 0.048 | 145 ± 50.0 | 0.010 ± 0.0035 | 6.05 ± 2.09 | 0.879 ± 0.037 | |

**Table 2.** Events of elevated trace gas concentrations at the CRV tower due to fire emissions. Columns show the number of 30 s measurements used to calculate emission factors for each event (N), the time of the event, emission ratios (ppmv ppmv$^{-1}$), emission factors (g per kg biomass combusted), and modified combustion efficiency (MCE). Dominant combustion phase is described as flaming, mixed, or smoldering.

| | Fire Name | Distance (km) | Contribution (%) | Total Hectares | Fuel Type | Ignition Source | |
|---|---|---|---|---|---|---|---|
| 1 | Tozitna | 229 | 10.7 | 31652 | Black Spruce | Lightning | |
| 2 | Kobe | 119 | 7.20 | 3444 | Black Spruce | Lightning | |
| 3 | Blair | 82 | 6.31 | 15217 | Black Spruce | Lightning | 5 |
| 4 | Aggie Creek | 41 | 5.63 | 12829 | Black Spruce | Lightning | |
| 5 | Spicer Creek | 195 | 5.30 | 39761 | Black Spruce | Lightning | |
| 6 | Blind River | 252 | 3.87 | 24608 | Black Spruce | Lightning | |
| 7 | Holtnakatna | 404 | 3.44 | 90308 | Mixed | Lightning | |
| 8 | Blazo | 514 | 3.39 | 49106 | Black Spruce | Lightning | |
| 9 | Big Creek 2 | 351 | 3.23 | 126637 | Black Spruce | Lightning | |
| 10 | Chitanana River | 241 | 3.12 | 17483 | Black Spruce | Lightning | 10 |
| 11 | Sea | 309 | 3.06 | 172 | Black Spruce | Human | |
| 12 | Sushgitit Hills | 276 | 2.92 | 111712 | Black Spruce | Lightning | |
| 13 | Big Mud River 1 | 254 | 2.72 | 42076 | Black Spruce | Lightning | |
| 14 | Lost River | 347 | 2.58 | 21088 | Black Spruce | Lightning | |
| 15 | Munsatli 2 | 302 | 2.36 | 40682 | Black Spruce | Lightning | |
| 16 | FWA Small Arms Complex | 19 | 2.31 | 740 | Black Spruce | Prescribed | 15 |
| 17 | Tobatokh | 280 | 2.24 | 21868 | Black Spruce | Lightning | |
| 18 | Trail Creek | 363 | 2.24 | 11939 | Black Spruce | Lightning | |
| 19 | Lloyd | 201 | 2.22 | 26818 | Black Spruce | Lightning | |
| 20 | Isahultila | 342 | 2.17 | 60445 | Black Spruce | Lightning | |
| 21 | Nulato | 499 | 2.17 | 449 | Black Spruce | Lightning | |
| 22 | Three Day | 472 | 2.17 | 39378 | Black Spruce | Lightning | 20 |
| 23 | Hay Slough | 188 | 1.90 | 37007 | Black Spruce | Lightning | |
| 24 | Rock | 316 | 1.83 | 3714 | Other | Lightning | |
| 25 | Sulukna | 329 | 1.77 | 6760 | Black Spruce | Lightning | |
| 26 | Titna | 273 | 1.77 | 12415 | Black Spruce | Lightning | |
| 27 | Quinn Creek | 657 | 1.49 | 2002 | Other | Lightning | |
| 28 | Harper Bend | 188 | 1.45 | 17555 | Black Spruce | Lightning | |
| 29 | Hard Luck | 328 | 1.43 | 5230 | Black Spruce | Lightning | 25 |
| 30 | Fox Creek | 369 | 1.42 | 2346 | Black Spruce | Lightning | |
| 31 | Bering Creek | 280 | 1.36 | 45654 | Black Spruce | Lightning | |
| 32 | Eden Creek | 324 | 1.16 | 18614 | Black Spruce | Lightning | |
| 33 | Falco | 390 | 1.10 | 1817 | Mixed | Lightning | |
| 34 | Jackson | 202 | 1.00 | 2969 | Black Spruce | Lightning | |
| 35 | Dulbi River | 404 | 0.95 | 22057 | Black Spruce | Lightning | 30 |

**Table 3.** All fires that contributed to at least 1% of the total CO anomaly observed at CRV tower ordered by largest CO
contribution. The distance column represents the distance of the center of the fire perimeter to CRV tower. Contribution is the
percent contribution to the total integral of fire CO at CRV for the entire 2015 fire season. Some fires were grouped together if
they were inside the same 0.5° grid cell during model coupling. For those cases, individual fire contribution to the CO anomaly
35   observed at CRV tower was weighted based on fire size.

40